Probing Achiral Benzene-1,3,5-tricarboxamide Monomers as Inducers of Homochirality in Supramolecular Helical Catalysts**

Huanjun Kong, Yan Li, Ahmad Hammoud, Ludovic Dubreucq, Claire Troufflard, Régina Maruchenko, Laurent Bouteiller, Matthieu Raynal

ChemistryEurope
Excellence in Chemistry Research Worldwide

Research Article
doi.org/10.1002/ceur.202300027

www.journal.chemistry-europe.org

Probing Achiral Benzene-1,3,5-tricarboxamide Monomers as Inducers of Homochirality in Supramolecular Helical Catalysts**

Huanjun Kong[+], Yan Li[+], Ahmad Hammoud, Ludovic Dubreucq, Claire Troufflard, Régina Maruchenko, Laurent Bouteiller, and Matthieu Raynal*[a]

Adding a complementary achiral monomer to polymers embedding a mixture of enantiopure monomers (the "sergeants") and achiral monomers (the "soldiers") is expected to decrease the optical purity of the polymer main chain. This study reports the influence of such achiral benzene-1,3,5-tricarboxamide (BTA) additives on the properties of "sergeants-and-soldiers" mixtures composed of an achiral BTA ligand coordinated to copper and of an enantiopure BTA monomer. Whilst *N*,*N*′,*N*″-tris(octyl)benzene-1,3,5-tricarboxamide (**BTA C8**) shows no significant improvement in term of enantioselectivity in the catalytic reaction of reference, achiral BTA monomers derived from α,α′-disubstituted amino esters all lead to an increase in the selectivity at low "sergeant" ratio. This different behaviour was probed by characterizing the coassemblies embedding **BTA C8**, i.e. the worst-performing achiral additive, and the BTA derived from the ester of 1-aminocyclohexane carboxylic acid (**BTA Achc**), the best-performing one. Both additives were found to efficiently intercalate with the ligand and the "sergeant" leading to the formation of single helices. However, only the terpolymer embedding **BTA Achc** appears to be homochiral, accounting for the good enantioselectivity even at very low "sergeant" ratio (0.25 %).

Introduction

Reacting monomers of different nature is well-established methodology to tune the properties, including chirality, of covalent macromolecules. In the realm of supramolecular polymers, it is achieved with lower synthetic efforts by the coassembly of complementary monomers interacting through non-covalent interactions upon selecting the convenient solvent that triggers the aggregation process.[1,2] It comes with additional challenges associated with lack of control of polymerization reaction and the difficulty to characterize the structure of the resulting copolymers.[3–5] Better control of the microstructure was achieved recently by triggering the assembly of kinetically-trapped species,[6–8] but achieving structural control under thermodynamic equilibrium is also necessary for many applications.[9] In the latter case, the degree of association and the length of the copolymers will strongly depend on the various equilibrium constants at work in the system as well as the mechanism of polymerization.[10,11] Mixing achiral monomers (the "soldiers") and chiral monomers (the "sergeants") is the most widespread strategy to generate homochiral helices, and probe the structure and stability of the resulting copolymers.[12–14] Thanks to the so-called "sergeants-and-soldiers" effect,[15] a few percent of "sergeant" molecules are usually enough to get single-handed helices, notably for copolymers derived from disc-like molecules such as benzene-1,3,5-tricarboxamides (BTAs).[16,17] In most of these systems, chiral and achiral monomers have roughly similar (co-)equilibrium constants leading to copolymers with a presumably random distribution of the monomers.[18] However, recent studies[5] demonstrated that subtle differences in these constants for cooperative supramolecular polymer assembly are key to manipulate the length and degree of association,[19–24] as well as the composition and monomer sequence[25–28] in the copolymers, with deep consequences on their rheological[20] and catalytic properties.[24] Recording the variation of the copolymer structural parameters under various conditions, *e.g.* temperature and concentration, fitted with thermodynamic mass-balance models, may allow to determine the role of the "sergeant" a posteriori,[23] but no design of the "sergeant" can be made a priori. In specific cases, it was found that the role of the "sergeant" could be modified by the effect of light[21] or chemical reactivity.[29] It would thus be highly advantageous to modify the structure and properties of "sergeants-and-soldiers" (S&S)-type copolymers by addition of a third component, that would be able to induce the desired functions to the multicomponent architecture.[30,31]

Water was recently shown to be able to intercalate into hydrogen-bonded assemblies of biphenyl tetracarboxamides in alkanes, leading to S&S-type polymers with tuneable and multiple helical states.[32,33] Desolvation of monomer side chains

[a] *H. Kong,[+] Dr. Y. Li,[+] Dr. A. Hammoud, L. Dubreucq, C. Troufflard, R. Maruchenko, Dr. L. Bouteiller, Dr. M. Raynal*
Sorbonne Université, CNRS, Institut Parisien de Chimie Moléculaire
Equipe Chimie des Polymères, 4 Place Jussieu, 75005 Paris (France)
E-mail: matthieu.raynal@sorbonne-universite.fr

[+] *These authors contributed equally to this work.*

[**] *A previous version of this manuscript has been deposited on a preprint server (https://doi.org/10.26434/chemrxiv-2023-n7m58).*

Supporting information for this article is available on the WWW under https://doi.org/10.1002/ceur.202300027

Research Article
doi.org/10.1002/ceur.202300027

may also play a key role in biasing and inverting the screw sense of hydrogen-bonded supramolecular (co)-polymers.[34,35] In addition to these intriguing effects displayed by small molecules, it seems opportune to use a third component for which the amount can be precisely tuned. Along our interest in developing the catalytic properties of supramolecular BTA coassemblies,[36–41] we recently disclosed that the extent of the S&S-effect was increased by two orders of magnitude, reaching homochirality with as low as 0.5% of "sergeants" and close to the optimal enantioselectivity, at the surprizing condition that an achiral BTA monomer was added to the catalytic mixture.[39] Improvement of the catalytic enantioselectivity at very low fraction of "sergeants" was observed in both the copper-catalyzed hydrosilylation[39] and hydroamination[40] reactions. The counterintuitive property of this BTA additive, derived from the ester of 1-aminocyclohexane carboxylic acid (**BTA Achc**, Scheme 1), to induce homochirality in supramolecular helical catalysts was attributed to its ability to stabilize the coassemblies and to suppress helix reversals, i.e. the conformational defects present in the pristine copolymers.[39] Herein, we probe whether similar improvements in the catalytic and chiroptical properties of the S&S-type helical catalysts can be induced by means of other achiral BTA additives. Our study reveals that enhancement of the S&S effect is not restricted to **BTA Achc** and that playing on the nature of the additive and its amount offers a good compromise to tune the extent of the S&S effect without jeopardizing the optimal selectivity of the terpolymer in the catalytic reaction of reference.

Results

Selection and synthesis of the achiral BTA monomers

Our aim was to evaluate achiral BTA monomers with sufficiently different structures to be able to determine key structural parameters that are needed to improve the extent of the S&S effect. We have selected *N*,*N*′,*N*″-tris(octyl)benzene-1,3,5-tricarboxamide (**BTA C8**), given its simple structure and its widespread use as a "soldier" in S&S-type experiments,[18,42,43] as well as **BTA Achc**[39] and other BTAs derived from α,α′-disubstituted amino esters (Scheme 1). These ester BTAs, that contain geminal methyl groups (**BTA Aib**),[44] cyclobutyl (**BTA Acbc**), cyclopentyl (**BTA Cle**) and cyclohexyl (**BTA Achc**) moieties connect to the amide functions, are named according to the nomenclature of the amino acid they originate from.[45] The new BTA derivatives, **BTA Acbc** and **BTA Cle**, have been synthesized and characterized by conventional techniques (see the Experimental Section). All BTAs derived from α,α′-disubstituted amino esters form hydrogen-bonded stacks in the solid state as probed by Fourier-Transform Infrared (FTIR) spectroscopy (see the Supporting Information).

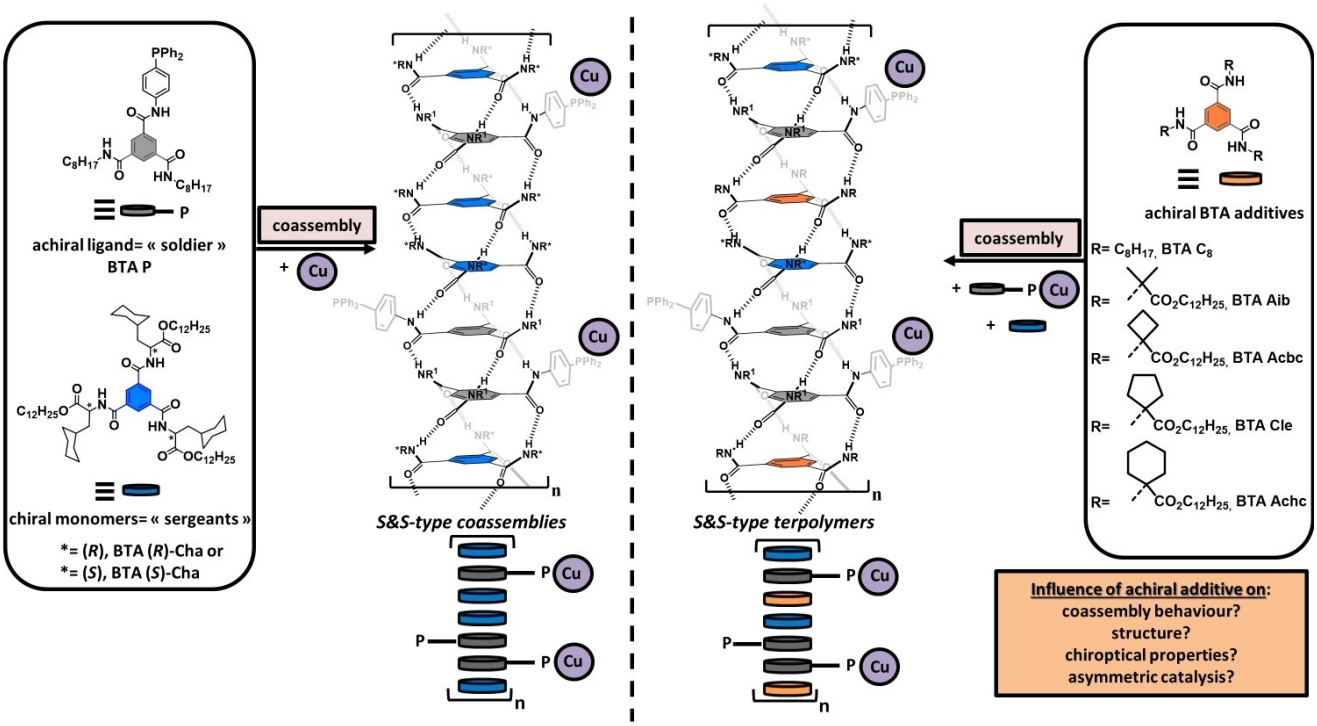

Scheme 1. Molecular structures of the BTA monomers, **BTA P** as "soldier", **BTA (*R*)-Cha** or **BTA (*S*)-Cha** as "sergeant" and various achiral BTAs tested as additives, used in this study and schematic representation of the two-component (coassemblies) and three-component (terpolymers) S&S-type assemblies formed without (left) and with (right) achiral additive. Supramolecular assemblies are represented as single helices for the sake of simplification (see the text for more details). The influence of the achiral BTA additive is particularly strong for mixtures containing low fractions of "sergeants" (i.e. **BTA (*R*)-Cha** or **BTA (*S*)-Cha**), quantified as $fs^0 = [\text{BTA Cha}]/([\text{BTA Cha}] + [\textbf{BTA P}] + [\text{achiral additive}])$, with [BTA Cha], [BTA P] and [achiral additive] being the concentrations of the respective components in the solution. In this study, **BTA P**·[Cu] refers to both free **BTA P** and BTA coordinated to $[Cu(OAc)_2 \cdot H_2O]$.

Research Article
doi.org/10.1002/ceur.202300027

Preliminary characterization of the supramolecular terpolymers composed of BTA C8 or BTA Achc

A crucial parameter for tuning the structure and properties of S&S-type coassemblies is that the achiral BTA monomer undergoes social sorting, i.e. it incorporates efficiently within the assemblies formed by the "sergeant" and the "soldier". The two-component coassemblies formed by **BTA P** coordinated to $[Cu(OAc)_2 \cdot H_2O]$ (**BTA P**·[Cu]), the catalytically-active "soldier", and **BTA Cha**, the enantiopure monomer acting as "sergeant", were previously probed by multifarious techniques.[37,38,41] **BTA Cha**, even if it forms dimers on its own,[46] intercalates very efficiently within the stacks of **BTA P** (see a schematic representation in Scheme 1).[24] Previously reported FTIR data of the three-component mixture composed of **BTA P** coordinated to $[Cu(OAc)_2 \cdot H_2O]$, **BTA Cha** and **BTA Achc** unambiguously demonstrated full coassembly of the three partners within the same helices,[39] despite the fact that only **BTA P** is able to form hydrogen-bonded stacks on its own (Figures 1a and S1–S3). We now check whether **BTA C8**, the most structurally simple BTA

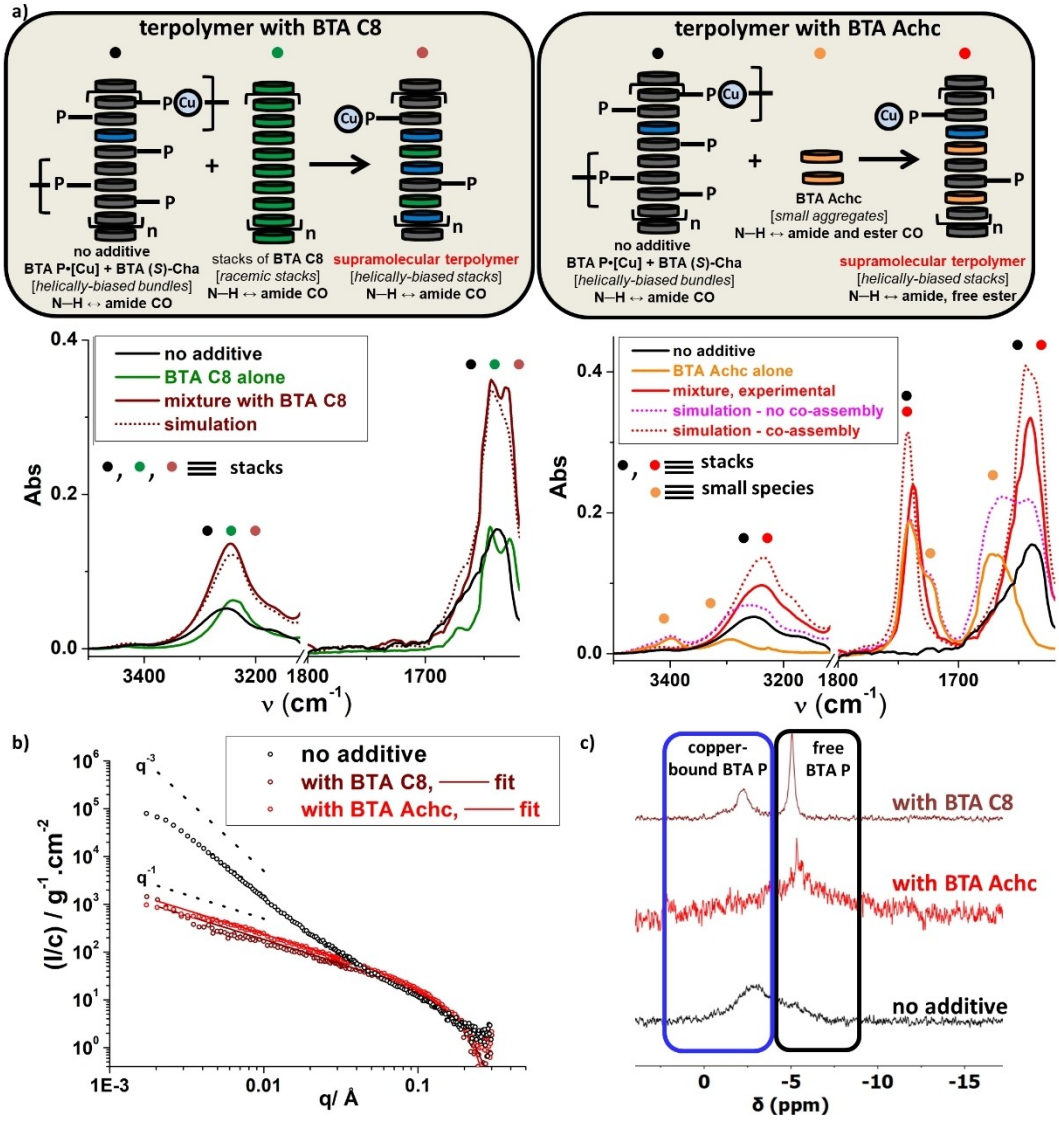

Figure 1. Preliminary characterization of the supramolecular terpolymers composed of **BTA C8** or **BTA Achc** (293 K except for NMR: 300 K, C_7D_8 or toluene). a) FTIR analyses of mixtures composed of **BTA P**·[Cu] (5.8 mM, **BTA P**/$[Cu(OAc)_2 \cdot H_2O] = 4$), **BTA (*S*)-Cha** (0.030 mM, $fs^0 = 0.25\,\%$ and $0.5\,\%$ with and without additive, resp.) without additive or with additives: **BTA C8** (5.8 mM, left) or **BTA Achc** (5.8 mM, right). For the three-component mixture with **BTA C8**, simulations for no and full coassembly both give the same result (see the main text and the Experimental Section for more information). For the three-component mixture with **BTA Achc**, simulated spectra are shown for no coassembly (i.e. segregation of the three partners) and full coassembly (i.e. social sorting of the three partners). The coassembly process towards supramolecular terpolymers is sketched above the FTIR spectra. b) Scattered intensity (cm^{-1}) normalized by the total BTA concentration for the mixtures composed of **BTA P·[Cu]** (3.95 ± 0.05 g.L^{-1}, 5.8 ± 0.1 mM, **BTA P**/$[Cu(OAc)_2 \cdot H_2O] = 4 \pm 0.2$), **BTA (*S*)-Cha** ($0.68 \pm 0.01$ g.L^{-1}, 0.58 ± 0.01 mM, $fs^0 = 6.2\,\%$ and $9\,\%$ with and without additive, resp.) without additive or with additives: **BTA C8** (1.6 g.L^{-1}, 3.0 mM) or **BTA Achc** (3.3 g.L^{-1}, 3.0 mM). SANS curves without additive[41] and with **BTA Achc**[39] have been reported previously. The three-component mixture containing **BTA C8** is fitted similarly to the one containing **BTA Achc**, i.e. by considering that all BTA molecules are present in stacks (see the main text and the Experimental Section for more information). SANS analyses for the individual partners are shown in Figure S3. c) $^{31}P\{^1H\}$ NMR analyses of solutions having similar compositions to those of Figure 1b.

Research Article
doi.org/10.1002/ceur.202300027

additive of our series, can undergo a similar behavior. FTIR, Small Angle Neutron Scattering (SANS), and Nuclear Magnetic Resonance (NMR) analyses of the mixtures composed of **BTA P·[Cu], BTA (*S*)-Cha** and **BTA C8** or **BTA Achc** as BTA additives have thus been performed for mixtures containing a small (a few percent) and very small quantity (a few tenth of a percent) of **BTA (*S*)-Cha**, since the influence of the achiral additive was found to be the most striking for the "sergeant"-poor mixtures. **BTA C8** or **BTA Achc** exhibit drastically different self-assembly behavior in toluene since long stacks and small aggregates have been identified for the former and the latter, respectively, consistently with the literature[39] and the data herein (Figures 1a, S1–S3). However, it is not clear whether this difference in self-assembly behavior will impact their ability to intercalate with the S&S-type coassemblies composed of **BTA P·**[Cu] and **BTA (*S*)-Cha**.

FTIR analyses of the three-component mixtures embedding a very small quantity of **BTA (*S*)-Cha** ($fs^0 = 0.25\,\%$) and **BTA C8** or **BTA Achc** as achiral additives are shown in Figure 1a. Please note that in this manuscript, the fraction of the "sergeants" (**BTA (*S*)-Cha** or **BTA (*R*)-Cha**) will be reported against the concentrations of both achiral monomers, i.e. **BTA P·**[Cu] (the "soldier") and the achiral BTA additive if any (see the formula of fs^0 in the caption of Scheme 1). FTIR spectrum of the coassemblies with **BTA C8** is characteristic of amide-bonded monomers present in long BTA stacks, with maxima at $\nu \approx 3240\ cm^{-1}$ and $\nu \approx 1640\ cm^{-1}$ for bonded N–H and C=O respectively, but social sorting or segregation cannot be disentangled here as both **BTA C8** on its own and S&S-type coassemblies exhibit similar FTIR patterns. It is worth noting that it is not possible to quantify the amount of **BTA (*S*)-Cha** actually present in the stacks given the very low amount present in the mixture. FTIR analysis of a three-component mixture containing a higher fraction of **BTA (*S*)-Cha** ($fs^0 = 4.5\,\%$) displays similar bands but here it can be estimated that most of **BTA (*S*)-Cha** monomers ($70 \pm 20\,\%$) are incorporated into the stacks. However, this is true for both mixtures lacking or embedding **BTA C8** (Figure S1). The formation of supramolecular terpolymers with **BTA C8** cannot be ascertained at this stage. On contrary, similar FTIR analyses on three-component mixtures containing **BTA Achc** as achiral additive unambiguously confirm full coassembly, i.e. the formation of a supramolecular terpolymer in which all monomers are connected through amide bonds in stacks, since FTIR bands specific to small aggregates of **BTA Achc** or **BTA (*S*)-Cha** cannot be detected and simulated spectra for full co-assembly are in fair agreement with the experimental ones (Figures 1a and S2).[47]

SANS and $^{31}P\{^1H\}$ NMR analyses of three-component mixtures provide more insight in the coassembly process between S&S-type coassemblies and **BTA C8**. The q^{-1} dependency of the scattering intensity at moderate q values is consistent with the presence of cylindrical objects for mixtures with and without **BTA C8** or **BTA Achc** (Figure 1b). However, while the mixture without achiral BTA additive exhibits a significant deviation of the q^{-1} dependency at low q values indicative of the presence of crosslinked cylinders, the additive-containing mixtures show no (for **BTA Achc**) or very limited (for **BTA C8**) deviation. Our recent in-dept characterization of the effect of copper on the structure of S&S-type coassemblies reveals that copper atoms act as crosslinkers between BTA helices when the fraction of "sergeant" in the stacks is below 20 %, as in the present case.[41] The SANS data reported herein demonstrate that the copper crosslinks are largely absent even for "sergeant"-poor mixtures when **BTA Achc** or **BTA C8** are added in the mixture. The absence of crosslinks is even more remarkable considering that the concentration of BTA molecules in the additive-containing mixtures is higher than in the additive-free mixture and probably results from the increased steric hindrance around the copper atoms. A consistent fit of the SANS data for additive-containing mixtures is obtained by assuming that all BTA molecules assemble in the same rigid rods of infinite length. The obtained radius of 12.1 Å and 11.0 Å, for **BTA Achc** and **BTA C8** mixtures, respectively, are consistent with a single molecule being present in the cross-section of coassemblies, i.e. single helices (Table 1). The remarkable different SANS signatures between the mixtures lacking or containing **BTA C8** unambiguously reveal that **BTA C8** is at least partly integrated into the coassemblies composed of **BTA P·**[Cu] and **BTA (*S*)-Cha**, i.e. that supramolecular terpolymers form similarly to what was previously observed for coassemblies with **BTA Achc**.[39]

^1H NMR analyses dot not allow to detect any major differences between additive-free and additive-containing mixtures (Figure S4). However, $^{31}P\{^1H\}$ NMR proved to be a good probe of the rate of exchange of copper atoms between free **BTA P** and **BTA P** coordinated to $[Cu(OAc)_2 \cdot H_2O]$ centers in our helical BTA assemblies. In additive-free coassemblies, the exchange rate is slow relatively to the ^{31}P NMR frequencies of free and copper-bound **BTA P** leading to a broad asymmetric signal ($\delta_{max} \approx -3$ ppm, Figure 1c).[41] Drastically different ^{31}P NMR traces are observed in the same region for additive-containing mixtures. The ^{31}P signal for the supramolecular terpolymers incorporating **BTA Achc** appears to be by far the broadest one of the series, with a maximal intensity close to the frequency corresponding to free **BTA P**. The significant broadening of the signal might result from the increased stability of the assemblies that limit the motions of the PPh_2 groups and prevent average conformations (see below). ^{31}P analysis of the three-component mixture with **BTA C8** shows two clearly distinguishable signals that correspond to free and copper-bonded **BTA P**. A similar ^{31}P NMR pattern was observed previously for "sergeant"-rich S&S-type coassemblies without achiral additive, and it was attributed to a very slow exchange of copper atoms between free **BTA P** and copper-bound **BTA P** centers because of their separation by a large number of "sergeants".[41] The same explanation seems plausible here in

Table 1. Radius (r), linear density (n_L), and number of BTA molecules in the cross-section of the rods (n) deduced from the fit of the SANS data.

	r [Å]	n_L [$Å^{-1}$]	n
BTA C8 alone	8.5	0.31	1.1
mixture with BTA C8	11.0	0.23	0.82
mixture with BTA Achc	12.1	0.22	0.81

Research Article
doi.org/10.1002/ceur.202300027

which **BTA C8** monomers play the role of the intercalator between free and copper-bound **BTA P** monomers in the coassemblies. Moreover, similar ^{31}P NMR patterns are observed for solutions embedding a small quantity of "sergeants", further corroborating the efficient intercalation of the achiral additives (Figure S4).

In overall, the aforementioned analyses reveal similar spectroscopic features for mixtures imbedding **BTA Achc** and **BTA C8** and demonstrate the possibility to generate supramolecular terpolymers for which catalytically performance can be different from that exhibited by additive-free copolymers.

Catalytic evaluation of the supramolecular terpolymers

S&S-type mixtures were evaluated in the copper-catalyzed hydrosilylation of 4-nitroacetophenone (NPnone) in toluene at 200 K and [**BTA P**] = 16.1 mM, conditions under which homochiral BTA helical catalysts yield the catalytic product, 4-nitroacetophenol (NPnol), with good enantioselectivity.[39] In absence of achiral BTA additive (black curve in Figure 2a), coassemblies provide NPnol in >95% enantiomeric excess (*e.e.*) at the condition that a high amount of **BTA (*S*)-Cha** is present in the mixture (96% *e.e.* for $fs^0 = 35\%$, maximal value of 97% *e.e.* reached for $fs^0 = 52\%$). The S&S-effect is thus moderate, yet it is better at 200 K than observed at 293 K in our previous report for which a fs^0 value >52% was required to get optimal selectivity.[39] This is a probable consequence of the reduction of the number of chiral defects in the S&S-type assemblies at low

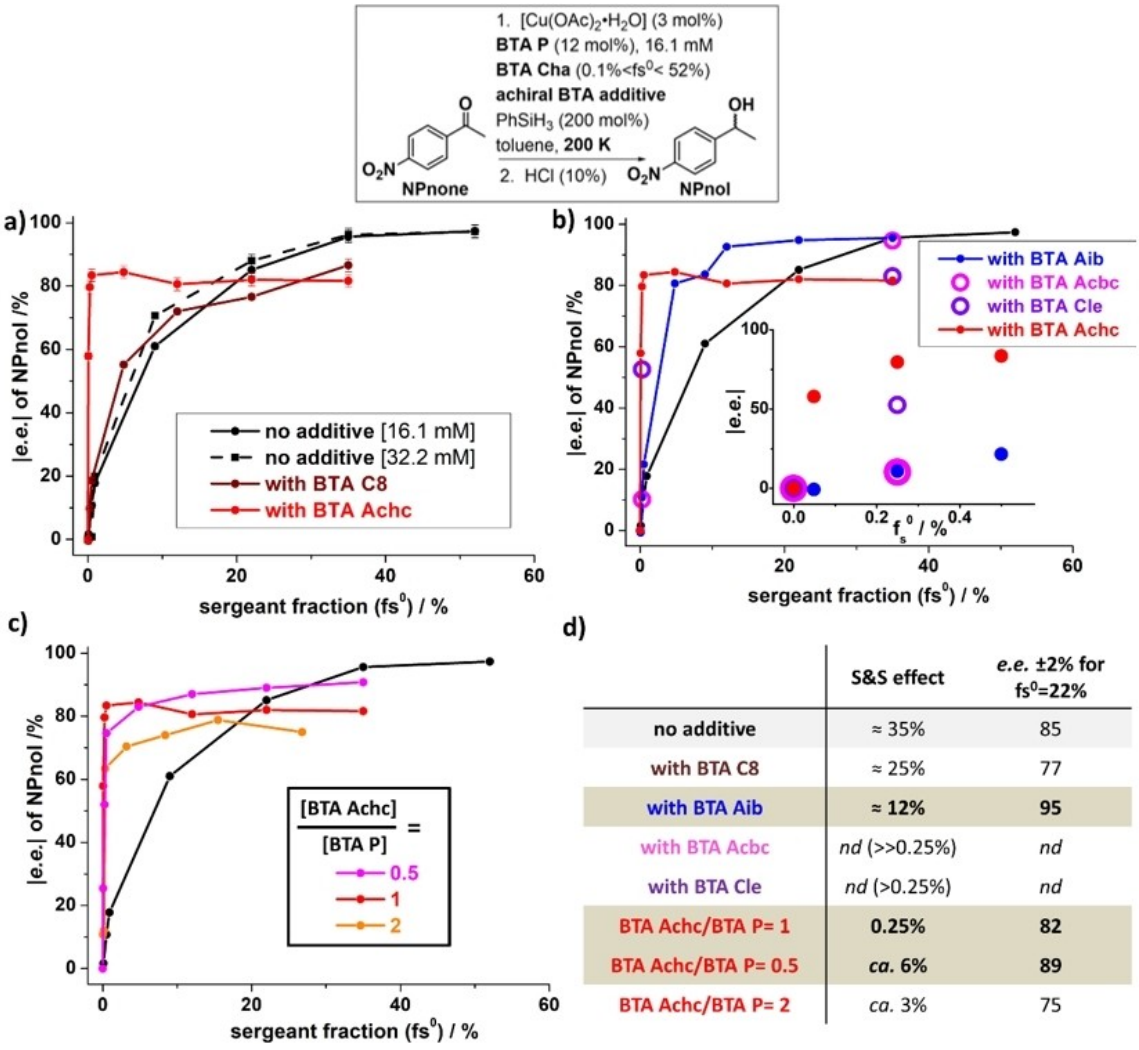

	S&S effect	*e.e.* ±2% for fs^0=22%
no additive	≈ 35%	85
with BTA C8	≈ 25%	77
with BTA Aib	≈ 12%	95
with BTA Acbc	*nd* (>>0.25%)	*nd*
with BTA Cle	*nd* (>0.25%)	*nd*
BTA Achc/BTA P= 1	0.25%	82
BTA Achc/BTA P= 0.5	*ca.* 6%	89
BTA Achc/BTA P= 2	*ca.* 3%	75

Figure 2. Catalytic evaluation of the effect of achiral BTA additives under the conditions indicated above the figure (conversion >99% in all cases). All *e.e.* values are plotted in Tables S1-S3. a) Plot of the *e.e.* in NPnol as a function of fs^0 for the S&S-type mixtures without achiral BTA additive and **with BTA C8** or **BTA Achc** ([achiral BTA]/[**BTA P**] = 1). b) Plot of the *e.e.* in NPnol as a function of fs^0 for the S&S-type mixtures embedding the different achiral BTA additives (([achiral BTA]/[**BTA P**] = 1). The plot for the mixture without additive (black) is shown for comparison. For **BTA Acbc** and **BTA Cle**, only a few catalytic mixtures have been evaluated that correspond to very low ($fs^0 = 0.25\%$) or high ($fs^0 = 35\%$) "sergeant" contents. Inset: zoom to distinguish the effect of achiral BTA additives at low fs^0 values. c) Plot of the *e.e.* in NPnol as a function of fs^0 for the S&S-type mixtures with different ratios of **BTA Achc** over **BTA P**. d) Table indicating the extent of the S&S effect and the enantioselectivity in NPnol (for $fs^0 = 22\%$) for the mixtures with and without additives. *nd*: not determined.

Research Article
doi.org/10.1002/ceur.202300027

temperature.[18] The influence of **BTA C8** and **BTA Achc**, in equimolar amount relatively to **BTA P**, was then probed.

BTA C8 exhibits a modest influence on the selectivity of the reaction relatively to the catalytic mixtures without additive (compare black and wine curves, Figure 2a). The higher *e.e.* values for $fs^0 < 10\%$ indicate a slight enhancement of the S&S effect, while *e.e.* values are lower than those of additive-free mixtures for high fs^0 values. The experimental selectivities can be compared to the ones that would be obtained for a putative achiral BTA additive acting as mere diluting agent, i.e. leading to a reduced number of **BTA P** molecules in the chiral environment in the coassemblies and coincidentally to lower enantioselective **BTA P**·[Cu] sites. The deviation of the experimental *versus* the simulated plot (Figure S5), with again higher *e.e.* values for $fs^0 < 10\%$ values and lower *e.e.* values at higher fs^0 values, indicate that **BTA C8** in supramolecular terpolymers is not simply an achiral intercalator but rather plays an active role in the induction of chirality, either slightly positively or negatively, to the catalytic centers (see below). Nonetheless, the influence of **BTA C8** on the selectively of the reaction over the full range of fs^0 values remains largely not beneficial.

In contrast, in presence of **BTA Achc** (red curve, Figure 2a), the selectivity reaches a plateau with as low as 0.25% of "sergeants" which corresponds to an enhancement of the S&S effect by two orders of magnitude. The drastic effect is not due to an increase in the total concentration in BTA monomers since increasing the concentration of S&S-type coassemblies without additive has no substantial effect on the selectivity (dashed black curve). This improvement of the S&S effect is accompanied by a decrease of the obtained selectivity which is of ca. 82% *e.e* on the plateau (i.e. 85% of the maximal selectivity that can be reached with these BTA helical catalysts). This is in full agreement with our previous catalytic evaluation made at 293 K.[39]

The influence of other achiral BTAs derived from α,α′-disubstituted amino esters is shown in Figure 2b. **BTA Aib** exhibits a clear enhancement of the selectivity with a plateau reached for 12% of "sergeants" and *e.e.* values of ca. 95%, very close to the maximal selectivity. The improvement of the S&S effect with **BTA Aib** is not as large as with **BTA Achc** but **BTA Aib** allows to reach higher *e.e.* values for mixtures with $fs^0 \geq 12\%$. Only a few catalytic mixtures were evaluated with **BTA Acbc** and **BTA Cle**. The influence of **BTA Acbc** on the selectivity seems similar to that of **BTA Aib**. A dramatic enhancement of the selectivity is seen with **BTA Cle**: 53% *e.e.* is reached with as low as 0.25% of "sergeants" in the mixture, yet this value is lower than that observed with **BTA Achc** at the same fs^0 value (79.6% *e.e.*). The selectivity at $fs^0 = 52\%$ is similar to that of **BTA Achc**, and thus no clear improvement is observed with **BTA Cle** relatively to **BTA Achc**. In overall, the following trend on the extent of the S&S effect in these catalytic experiments can be determined: **BTA Achc** > **BTA Cle** > **BTA Aib** ≈ **BTA Acbc** > **BTA C8** ≈ no additive whilst the maximal selectivity reached at high fs^0 values follows an almost opposite trend (**BTA Achc** ≈ **BTA Cle** < **BTA C8** < **BTA Aib** ≈ **BTA Acbc** ≈ no additive). It is remarkable that such subtle changes in the chemical structures of the achiral BTA additives impact drastically both the extent of chiral induction in the resulting supramolecular helical catalysts and the maximal selectivity.

The influence of the amount of **BTA Achc** relatively to **BTA P** was subsequently examined (Figure 2c). On the one hand, decreasing by two the amount of **BTA Achc** relatively to the previous experiment leads to a slight decrease of the selectivity at low fs^0 values but improved *e.e.* values at high fs^0. The selectivity plateau is reached for ca. 6% of "sergeants" that corresponds to ca. 89% *e.e.*, thus representing a significant improvement relatively to the use of an equimolar of **BTA Achc** (ca. 82% *e.e* on the plateau). On the other hand, doubling the amount of **BTA Achc** is detrimental for the selectivity whatever the fs^0 value.

In overall, the outcome of the catalytic experiments is compiled in the Table of Figure 2d and can be summarized as follows: i) all tested achiral BTA additives derived from α,α′-disubstituted amino esters lead to a significant improvement of the enantioselectivity of the catalytic reaction at low fs^0 values, but not **BTA C8**, ii) the optimal selectivity reached at the selectivity plateau also depends on the nature of the achiral BTA additive and appears to be inversely proportional to their ability to enhance the S&S effect, and iii) the extent of the S&S effect and the optimal selectivity can be tuned by playing on the nature of the achiral BTA additive and its amount relatively to **BTA P**; **BTA Aib** appears to offer a good compromise between these two desirable properties.

Rationalizing the different catalytic effects induced by BTA C8 and BTA Achc

Despite the previous spectroscopic data indicating that both **BTA C8** and **BTA Achc** are able to coassemble with **BTA P**·[Cu] and **BTA Cha** into single helices, only the supramolecular terpolymer embedding **BTA Achc** leads to significantly improved catalytic properties relatively to additive-free mixtures (Figure 2). Additional analyses were conducted to find the origin of the different behavior exhibited by the two supramolecular terpolymers. The macroscopic aspect of the corresponding solutions provides a first indication that the structure of these supramolecular terpolymers is by far not identical. Pictures of the solutions embedding low ($fs^0 = 9\%$) and very low ($fs^0 = 0.5\%$) quantity of "sergeants" with and without these additives are shown in Figure S6. Fifteen minutes after dissolution, all solutions are transparent but only those containing **BTA Achc** are viscous (see also the corresponding movies). After one day, the solution without additive appears turbid and slightly viscous, this is due to the formation of aggregated helices with copper atoms acting as crosslinkers as characterized in Figure 1b and discussed in our recent study.[41] The aspect of the solutions with **BTA Achc** and **BTA C8** remain similar to that observed after 15 minutes, i.e. viscous and fluid, respectively. The presence of entanglements between the supramolecular chains embedding **BTA Achc** are probably responsible for the increase in viscosity. This observation infers that supramolecular terpolymers containing **BTA Achc** are significantly longer than those containing **BTA C8**, an informa-

Research Article
doi.org/10.1002/ceur.202300027

tion that cannot be extracted from the aforementioned SANS analyses because of the limited range of the low q region.

Circular dichroism (CD) analyses provide another remarkable difference between these supramolecular terpolymers. The CD signal detected in the 275–350 nm region belongs exclusively to the "soldier", i.e. **BTA P**·[Cu], and thus corresponds to an induced CD band (ICD).[24,37–39,41] For coassemblies of **BTA P**·[Cu] and BTA Cha, the intensity of this ICD band is correlated to the enantioselectivity.[24,41] For the solution containing 9% of **BTA (*R*)-Cha** and analyzed at 293 K, the addition of **BTA C8** leads to a slightly more intense ICD signal relatively to the additive-free mixture (Figure 3a). This is consistent with the fact that these two mixtures display similar enantioselectivities (Figure S5), i.e. 61% *e.e.* and 55% *e.e.* for the mixtures with and without **BTA C8**, respectively, despite the fact that the solutions with **BTA C8** contains two times more of achiral BTA monomers. The extracted Kuhn anisotropy factors (g values)[48] at $\lambda = 295$ nm are equal to 4.1×10^{-4} and 2.9×10^{-4} for the mixtures with and without **BTA C8**, respectively, clearly indicating that the assemblies are not homochiral. In contrast, the CD spectrum of the mixture with **BTA Achc** resembles that of a "sergeant"-rich solution inferring that homochiral helices are present. The enhanced g value, $g = 7.2\times10^{-4}$, is consistent with the improved enantioselectivity in the catalytic reaction for the supramolecular polymer embedding **BTA Achc** (84% *e.e.*).[49] In addition, the chiroptical properties of the copolymer and the terpolymers do not change in presence of NPnone, the substrate of the reaction, indicating that the different catalytic

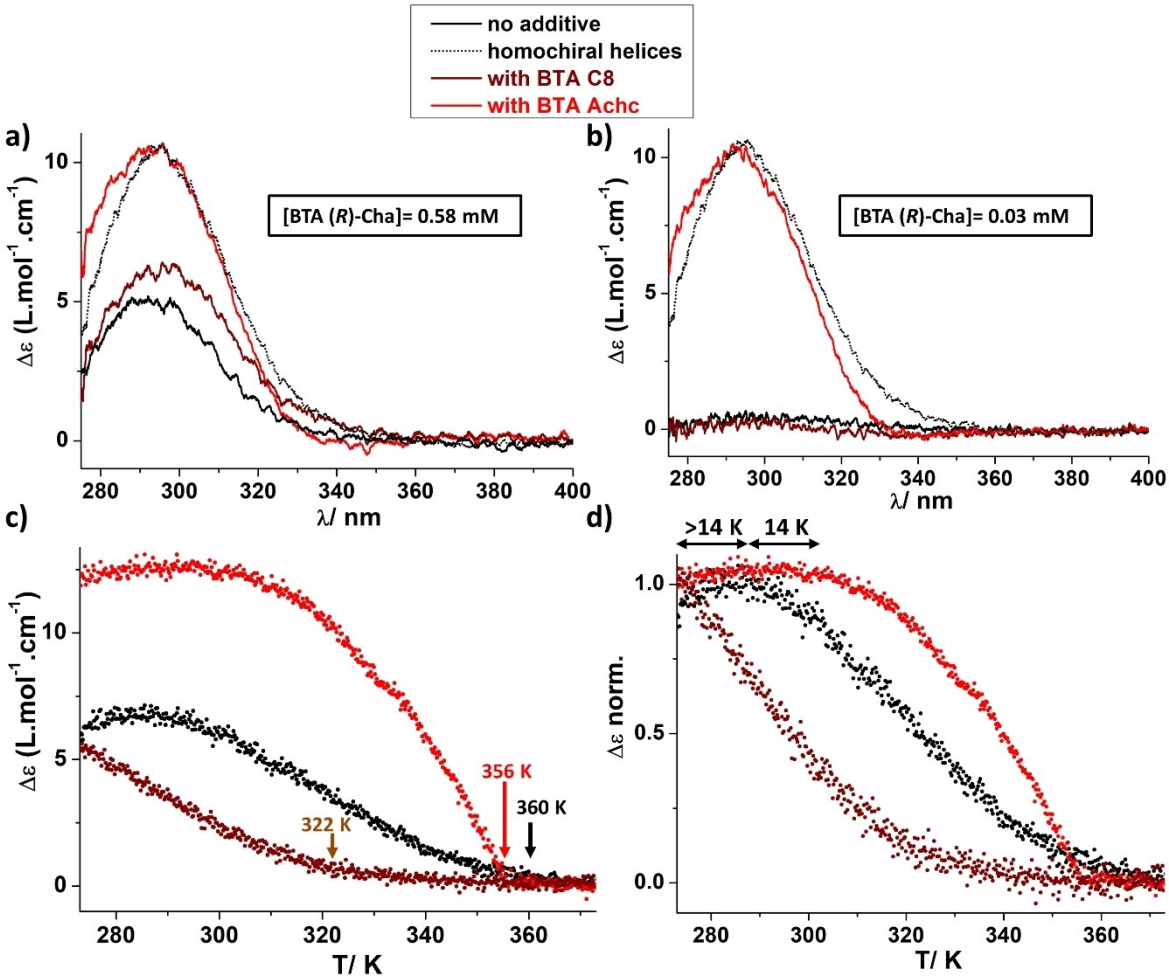

Figure 3. Evaluation of the effect of achiral BTA additives on the chiroptical properties of the supramolecular polymers (293 K, C_7D_8). a-b) Circular dichroism analyses of the solutions with and without achiral BTA additives, for mixtures containing 0.58 mM (a) or 0.030 mM (b) of **BTA (*R*)-Cha**. Composition for a): **BTA P**·[Cu] (5.8 mM, **BTA P**/[$Cu(OAc)_2\cdot H_2O$] = 4), **BTA (*R*)-Cha** (0.58 mM, $fs^0 = 4.7\%$ and 9% with and without additive resp.) without additive and with additives: **BTA Achc** (5.8 mM) or **BTA C8** (5.8 mM). Composition for b): **BTA P**·[Cu] (5.8 mM, **BTA P**/[$Cu(OAc)_2\cdot H_2O$] = 4), **BTA (*R*)-Cha** (0.03 mM, $fs^0 = 0.25\%$ and 0.5% with and without additive resp.) without additive and with additives: **BTA Achc** (5.8 mM) or **BTA C8** (5.8 mM). CD spectra of additive-free solution with $fs^0 = 52\%$ is selected as a signature of homochiral helices. c) Variable-temperature CD analyses of the solutions with and without achiral BTA additives (cooling curves (0.3 $K.min^{-1}$). The solutions have similar compositions to those in Figure 3a but those containing the achiral BTA additives have been diluted twice in order to maintain the total concentration in BTA monomers approximately constant. Total BTA concentration = 6.4 mM (without additive), 6.1 mM (with additives). The elongation temperatures for each curve is indicated by the arrows. d) Normalized variable-temperature CD data at the maximum molar circular dichroism value ($\triangle\varepsilon_{max}$). The difference in the thermal stability between the different polymers is indicated above the spectra and correspond to the difference between the critical temperatures at the onset of the $\triangle\varepsilon$ plateaus. For a-d), $\triangle\varepsilon$ is calculated by dividing the ellipticity values by 32982×[**BTA P**]×l where l corresponds to the CD cell pathlength (0.01 cm).

Research Article
doi.org/10.1002/ceur.202300027

performance of the polymers cannot be attributed to a specific interaction with the substrate (Figure S7).

The different behavior between the two achiral BTA additives is even more striking when these BTAs are added to mixtures containing a very small quantity of **BTA (*R*)-Cha** ($fs^0 =$ 0.5 %, Figure 3b). Under these conditions, additive-free and **BTA C8** containing mixtures are almost CD silent, i.e. the "sergeant" is not able to induce its chiral preference to the polymer main chain, leading to almost racemic helices that drive the reaction with poor level of enantioinduction (consistently with ca. 10 % *e.e.* obtained for both mixtures in the catalytic reaction). In contrast, an intense CD signal is observed upon addition of **BTA Achc**, the corresponding g value at 295 nm of 6.2×10^{-4} agrees with both almost homochiral helices and the high enantioselectivity (80 % *e.e.*), despite the very small quantity of "sergeants" in the supramolecular terpolymer. The drastically different catalytic outcome induced by **BTA Achc** and **BTA C8** to "sergeant"-poor helical coassemblies can thus be suitably rationalized by the chiroptical properties of the resulting supramolecular terpolymers.

Spectroscopic data were analyzed into more details in order to detect any additional differences induced by the BTA additives. ICD signals exhibit very similar shapes even though those enhanced or induced by **BTA Achc** appear to be slightly blue-shifted (Figure S8). This is also valid for UV-Vis signals in the same region except that here both those of **BTA Achc** and **BTA C8** appear slightly blue-shifted relatively to additive-free polymers. FTIR signals relative to hydrogen-bonded amide functions in the supramolecular terpolymers have been compared to those of their individual components. **BTA Aib** (a blue print of the FTIR signature of **BTA Achc** in stacks) and **BTA C8** exhibit both a stronger and more regular hydrogen bonding network than **BTA P**·[Cu] as can be deduced from the frequencies and width of their corresponding amide N–H and C=O bands (Figure S9). However, amide functions in the supramolecular terpolymers seem to adopt an average conformation that perfectly matches the weighed contributions of each partner. It means that neither **BTA Achc** nor **BTA C8** seem to impose its preferential conformation to **BTA P**·[Cu] in the hydrogen bonding network. In overall, this set of analyses indicate that achiral additives do not significantly affect the nature of the hydrogen bonding network and the conformation of the PPh_2 groups in the coassemblies but rather play a role in eliminating the conformational defects, the latter property being most significantly achieved in the case of **BTA Achc** at low fs^0 values.

Finally, variable-temperature CD experiments have been conducted since these analyses provide additional information on the structure and stability of the supramolecular terpolymers.[11,23] Analyses have been performed by diluting the solutions with additives by two in order to keep the total concentration in BTA monomers approximatively constant (Figure 3c). Under these conditions, all coassemblies are disrupted at 373 K, as deduced from the absence of CD signal. It is worthy to note that the observation of a monotonic increase of the molar CD values upon cooling is consistent with all monomers being distributed in the supramolecular terpolymers. In addition, the supramolecular terpolymer embedding **BTA C8** exhibits lower molar CD values than the additive-free coassemblies over all the temperature range. The latter observation is probably due to the fact that the concentration in **BTA P**·[Cu] has been divided by two comparatively to CD analyses presented in Figure 3a. It has been previously observed that induction of chirality to **BTA P**·[Cu] is more difficult when experiments are conducted close the critical concentration of **BTA P**.[39] However, this dilution does not seem to affect the chiroptical properties of the supramolecular terpolymer containing **BTA Achc** as the molar CD value reached upon cooling is consistent with the formation of homochiral helices. Examination of the cooling curves reveals three major differences between the polymers (Figure 3c–d): i) the assembly of the BTA monomers in presence of **BTA Achc** is far more cooperative than with **BTA C8** or in absence of additive, as can be seen by the sudden (for **BTA Achc**) *versus* gradual (for additive-free and **BTA C8**) increase of the molar CD value at the respective elongation temperatures,[11] ii) the elongation temperatures are similar for **BTA Achc** and additive-free containing polymers but significantly higher (> 40 K) than the one of the **BTA C8** containing polymer, iii) the critical temperature at which the molar CD value reaches its maximal value increases in the following order: **BTA C8** $<$ no additive ($\triangle T > 14$ K) $<$ **BTA Achc** ($\triangle T > 28$ K relatively to **BTA C8** mixture). The higher stability of supramolecular terpolymer with **BTA Achc** may come in part from its homochiral nature (i.e. from the presence of fewer conformational defects) and the drastic difference in stability between the partially helically-biased polymers suggests that **BTA C8** significantly affects the stability of the coassemblies. All these observations demonstrate that **BTA Achc** and **BTA C8** interact differently with S&S-type coassemblies of **BTA P**·[Cu] and BTA Cha, leading to stabilization or destabilization of the polymers, respectively.

Discussion

Achiral additives are ubiquitous in asymmetric reactions performed with discrete catalysts as they may drastically influence the reaction outcome by modifying the structure of the catalyst or the transition state.[50] Their role in supramolecular chemistry is less established as they can compete with the existing non-covalent interactions between the molecules and destabilize the supramolecular structures.[51] In the realm of polymer sciences, chiral monomers act as "sergeants" that induce their chirality to a large number of achiral ones, "the soldiers", and thus allow macromolecules to be single handed, i.e. homochiral.[12–14] Adding achiral monomers in the main chain of such type of polymers will dilute the chiral influence of the "sergeant", and such a dilution process will lower the optical purity of the polymer when the ratio of the chiral monomer would be too low to sustain an optimal "sergeants-and-soldiers" effect. The fate of a macroscopic property, such as reaction enantioselectivity, that is correlated to the optical purity of the polymer, will be consequently affected.[52]

Research Article
doi.org/10.1002/ceur.202300027

In the present study, none of the tested achiral monomers added to the supramolecular BTA helical catalysts composed of **BTA P**·[Cu] and BTA Cha behave as a strict diluting agent at low fs^0 values (Figure S5). This indicates that a better transfer of the chiral preference of the "sergeant" is achieved when **BTA P** "soldiers" are replaced or mixed with these achiral additives. This suggests that imposing a chiral preference to **BTA P** is more difficult than to the tested additives. The weakly ordered hydrogen-bonding network of **BTA P** (Figure S8), as a probable result of its C_2-symmetry *versus* C_3-symmetry for the tested additives, may explain this behavior.[39] In addition, the ability of the additives to prevent the formation of copper crosslinked helices is also beneficial for the induction of chirality in the BTA assemblies.[41]

However, this enhancement of the "sergeants-and-soldiers" effect, leading to higher enantioselectivities for "sergeant"-poor mixtures relatively to additive-free catalysts, appears to be significant only for the additives derived from α,α′-disubstituted amino esters. The most impressive effect is seen for **BTA Achc**, with ca. 85% of the optimal selectivity reached with as low as 0.25% of "sergeants" but **BTA Aib**, derived from cheaper 2-aminoisobutyric acid, also displays a significant improvement. The maximal selectivity varies as a function of the nature of the achiral BTA additive, with a notable decrease in the case of **BTA Achc**. The origin of the non-maximal selectivity for the catalytic system in presence of **BTA Achc**, despite the formation of homochiral helices, is unclear for now. In a related catalytic system, employed in the copper-catalyzed hydroamination of styrene, **BTA Achc** was found to improve both the extent of the "sergeants-and-soldiers" effect and the enantioselectivity of the reaction, relatively to the additive-free catalyst.[40] For the hydrosilylation reaction reported in the present study, it is possible to play both on the nature of the achiral BTA additive and its amount in order to maintain an optimal selectivity (or close to it) even with a very small quantity of "sergeants" engaged in the catalytic system.

The similarities and differences between the assemblies of **BTA C8** and **BTA Achc**, the worst- and the best-performing achiral additives, respectively, are schematized in Figure 4. **BTA C8** exhibits the same ability as **BTA Achc** to intercalate into the stacks of **BTA P**·[Cu] and **BTA Cha**, preventing the formation copper crosslinked helices and leading to supramolecular terpolymers as single helices. These properties improve the extent of chirality induction in supramolecular BTA helices, but not drastically since only **BTA Achc** triggers the formation of homochiral helices when added to partly helically biased ones, or even to almost racemic helices. It is thus obvious that **BTA Achc** is able to remove conformational defects in the coassemblies,[53] as we previously quantified,[39] whilst **BTA C8** has only a limited effect on it. The induction and emergence of homochirality in the presence of **BTA Achc**, but not **BTA C8**, offers a good rationale of the outcome of the catalytic reaction. The present study also reveals that the assembly process is far more cooperative with **BTA Achc** and leads to longer and more stable supramolecular terpolymers. The different stabilities between **BTA C8** and **BTA Achc** terpolymers have not been reflected by the catalytic results, probably because catalytic tests have been performed at a high concentration of **BTA P** and at a low temperature, thus somewhat minimizing the negative influence of **BTA C8**. It is not clear yet how these

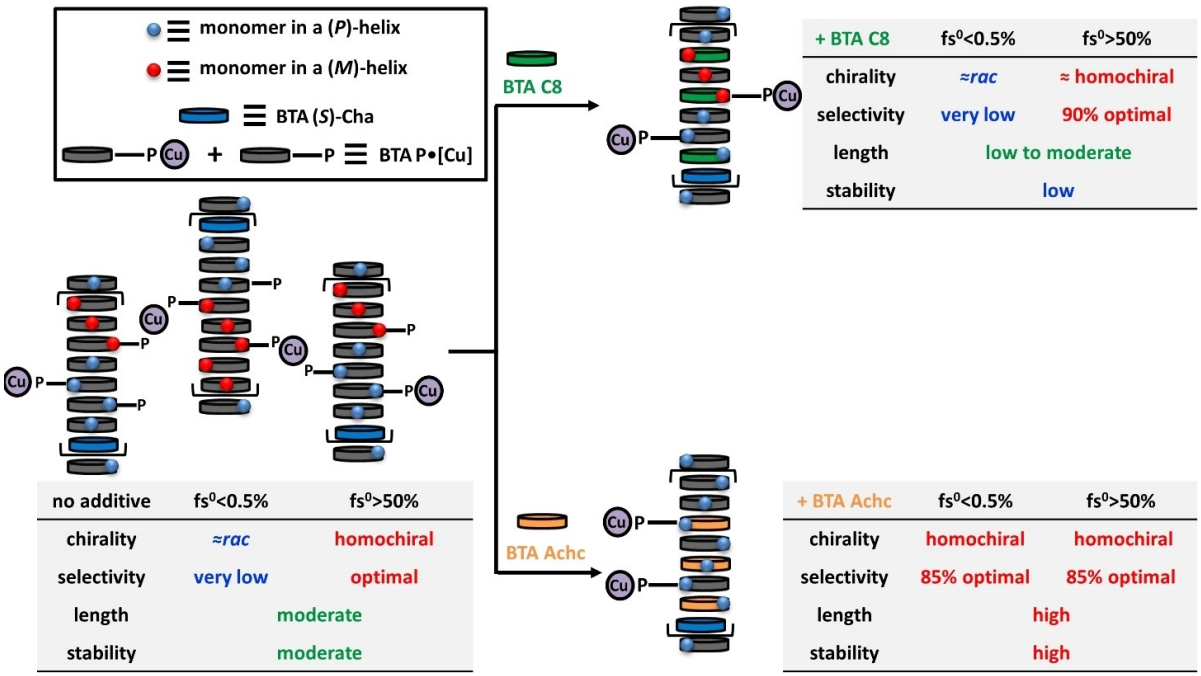

Figure 4. Schematic representation of the coassemblies without additive (left) and of the supramolecular terpolymers formed upon addition of **BTA Achc** or **BTA C8** (right). The main properties of these polymers with very small ($fs^0 = 0.5\%$) and high quantity of "sergeants" ($fs^0 > 50\%$) are compared in the respective tables.

Research Article
doi.org/10.1002/ceur.202300027

properties, i.e. cooperativity, length and stability, are connected to the emergence of homochirality, but it can be speculated that the induction of chirality may be facilitated into more rigid and longer assemblies *versus* more flexible and shorter ones. Whilst **BTA Achc** does not seem to change the nature of the hydrogen bond network and the conformation of the PPh_2 group of **BTA P** to a great extent, it remains to elucidate the exact sequence of the monomers in the terpolymers. It also remains to determine whether the side chains of **BTA Achc**, and potentially those of the other achiral additives, may influence the coordination sphere(s) of the metal catalyst, i.e. a local influence of the induction of chirality to the catalytic center rather than a distal control as in the present case.

Conclusion

The present study sheds more light on the counterintuitive ability of achiral benzene-1,3,5-tricarboxamide (BTA) monomers to improve the extent of the "sergeants-and-soldiers" (S&S) effect in BTA helical catalysis, allowing to get higher enantioselectivities in a catalytic reaction of reference. This improvement is not restricted to a single additive but rather a property shared by BTAs derived from α,α′-disubstituted amino esters. Intercalation and elimination of copper crosslinks, as observed for *N*,*N*′,*N*″-tris(octyl)benzene-1,3,5-tricarboxamide (**BTA C8**), is not a sufficient condition to significantly enhance the extent of chiral induction in supramolecular BTA helices. However, homochirality emerges from almost racemic helices in presence of the BTA derived from the ester of 1-aminocyclohexane carboxylic acid (**BTA Achc**), leading to optimal selectivity with only 0.25% of "sergeants" in the coassemblies, and this may be related to its ability to promote a cooperative association of the monomers into long and stable terpolymers. A better understanding on the origin of this particular effect could be beneficial from the design of better-performing helical BTA catalysts, with the ultimate goal of achieving perfect enantioinduction with minute amounts of chiral species.

Experimental Section

Materials: BTA P,[37] BTA Cha enantiomers,[44] **BTA Aib**,[44] **BTA C8**,[54] and **BTA Achc**[39] were synthesized as reported previously. **BTA (*S*)-Cha** and **BTA (*R*)-Cha** used in this study were purified by preparative HPLC as reported previously leading to optically-pure samples.[24] The dodecyl ester *p*-TsOH salts of 1-aminocyclobutane carboxylic acid (Acbc) and 1-aminocyclopenane carboxylic acid (cycloleucine, Cle) were prepared similarly to that of 1-aminocyclohexane carboxylic acid (Achc).[39] Acbc (97%, Sigma-Aldrich), Cle (97%, Sigma-Aldrich), 1-dodecanol (98%, Sigma-Aldrich), p-TsOH.H2O (≥98.5%, Sigma-Aldrich), benzene-1,3,5-tricarbonyl chloride (98%, Alfa Aesar), 4-nitroacetophenone (>98%, Alfa Aesar), $PhSiH_3$ (>97%, Alfa Aesar) and $[Cu(OAc)_2 \cdot H_2O]$ (>99%, Alfa Aesar) were used as received. Triethylamine (Aldrich) was distilled over CaH_2 prior to use. Dry THF, CH_2Cl_2 and toluene solvents were obtained from a Solvent Purification System (SPS). Acetone-d_6 and C_7D_8 were bought from Eurisotop and used without further purification. Purification by flash chromatography was performed by adsorbing the samples on silica; the adsorbed samples were introduced in the solid loader and purified by means of Reveleris X2 purification system (Buchi®) using pre-packed silica cartridges Ecoflex® (irregular 50 μm silica). A double wall glass beaker filled with PDMS (Kryo 90 from Lauda®) connected to cryostat Proline RP890 from Lauda® was used to perform the catalytic reactions at 200 K.

Methods for characterization of BTA Acbc and BTA Cle: NMR spectra were recorded on a Bruker Avance 300 spectrometer and calibrated to the residual solvent peak: acetone-d_6 (^{1}H: 2.05 ppm; ^{13}C: 29.84 ppm). Peaks are reported with their corresponding multiplicity (s: singlet; m: multiplet) and integration, and respective *J* coupling constants are given in Hertz. Exact mass measurements (HRMS) were obtained on TQ R30-10 HRMS spectrometer by ESI+ ionization and are reported in *m*/*z* for the major signal. FTIR spectra for solids were recorded by reflection on a Ge probe (attenuated total reflectance (ATR), see the Supporting Information) and the main bands were reported (w: weak, m: medium, s: strong, br: broad).

Methods for characterization of the supramolecular assemblies: Fourier-Transform Infrared (FTIR) analyses: FTIR measurements were performed on a Nicolet iS10 spectrometer. Spectra of solutions in toluene were measured in 0.02 cm pathlength CaF_2 cells at 293 K and were corrected for air, toluene and cell absorption (Figures S1 and S2). Procedure for simulated FTIR spectra (see Figures 1a, S1 and S2 for the results), the influence of the stack ends is neglected in all cases: Three-component mixture composed of **BTA P·[Cu]**, **BTA (*S*)-Cha** (0.58 mM, $fs^0 = 4.5\%$) and **BTA C8** (Figure S1): The concentration of dimers of **BTA (*S*)-Cha**[44,46] is presumed to be similar to that previously determined for the S&S-type coassemblies without **BTA C8**, i.e. mixture without achiral additive,[41] since both mixtures show similar FTIR traces in the 1720–1750 cm^{-1} region, region in which remaining **BTA (*S*)-Cha** dimers can be detected and quantified (Figure S1).[24,37–41] The amount of **BTA (*S*)-Cha** monomers in dimers and stacks is thus estimated to be 0.18 ± 0.13 mM and 0.40 ± 0.13 mM, respectively, that corresponds to 30 ± 20% and 70 ± 20% of **BTA (*S*)-Cha** introduced in the solution (the high uncertainty is due to the low intensity of the signals). The simulated spectrum is built by summing the FTIR spectra of these remaining **BTA (*S*)-Cha** dimers (0.18 mM), of **BTA P**·[Cu] (**BTA P** 5.8 mM + $[Cu(OAc)_2 \cdot H_2O]$ 1.45 mM), **BTA C8** (5.8 mM) and of **BTA Met**[43] (0.40 mM, in methylcyclohexane, used as blueprint of **BTA (*S*)-Cha** monomers in stacks). Three-component mixture composed of **BTA P·[Cu]**, **BTA (*S*)-Cha** (0.030 mM, $fs^0 = 0.25\%$) and **BTA C8** (Figure 1a): The amount of **BTA (*S*)-Cha** is too low to detect the corresponding signals. The simulated spectrum is built by summing the FTIR spectra of **BTA P**·[Cu] (**BTA P** 5.8 mM + $[Cu(OAc)_2 \cdot H_2O]$ 1.45 mM), of **BTA C8** (5.8 mM) and of **BTA Met**[43] (0.030 mM, in methylcyclohexane, used as blueprint of **BTA (*S*)-Cha** monomers in stacks). Three-component mixture composed of **BTA P·[Cu]**, **BTA (*S*)-Cha** (0.58 mM, $fs^0 = 4.5\%$) and **BTA Achc** (Figure S2): The concentration of remaining **BTA (*S*)-Cha** dimers cannot be determined precisely because both **BTA (*S*)-Cha** (0.58 mM) and **BTA Achc** (5.8 mM) absorb in the 1720–1750 cm^{-1} region. Simulations for both no (i.e. segregation) and full coassembly can be made in that case since **BTA (*S*)-Cha** and **BTA Achc** form dimers[44,46] and small aggregates[39] on their own, respectively. The simulated spectrum for segregation of the three partners in their own assemblies is built by summing their individual FTIR spectra, **BTA (*S*)-Cha** (0.58 mM), **BTA P**·[Cu] (**BTA P** 5.8 mM + $[Cu(OAc)_2 \cdot H_2O]$ 1.45 mM) and **BTA Achc** (5.8 mM). The simulated spectrum for full coassembly is built by summing the FTIR spectra of **BTA P**·[Cu] (**BTA P** 5.8 mM + $[Cu(OAc)_2 \cdot H_2O]$ 1.45 mM) of **BTA Met**[43] (0.58 mM, in methylcyclohexane, used as blueprint of **BTA (*S*)-Cha** monomers in stacks) and of **BTA Aib**[44] (5.8 mM, in methylcyclohexane, used as blueprint of **BTA Achc** monomers in stacks). Three-component

Research Article
doi.org/10.1002/ceur.202300027

mixture composed of **BTA P·[Cu]**, **BTA (*S*)-Cha** (0.030 mM, $fs^0 =$ 0.25%) and **BTA Achc** (Figure 1a): The simulated spectrum for segregation of the three partners in their own assemblies is built by summing their individual FTIR spectra, **BTA (*S*)-Cha** (extrapolated to 0.030 mM), **BTA P**·[Cu] (**BTA P** 5.8 mM + $[Cu(OAc)_2 \cdot H_2O]$ 1.45 mM) and **BTA Achc** (5.8 mM). The simulated spectrum for full coassembly is built by summing the FTIR spectra of **BTA P**·[Cu] (**BTA P** 5.8 mM + $[Cu(OAc)_2 \cdot H_2O]$ 1.45 mM) of **BTA Met**[43] (extrapolated to 0.030 mM, in methylcyclohexane, used as blueprint of **BTA (*S*)-Cha** monomers in stacks) and of **BTA Aib**[44] (5.8 mM, in methylcyclohexane, used as blueprint of **BTA Achc** monomers in stacks).

Small-angle neutron scattering (SANS) analyses: SANS measurements were made at the LLB (Saclay, France) on the PA20 instrument, at three distance-wavelength combinations to cover the 2×10^{-3} to 0.3 $Å^{-1}$ q-range, where the scattering vector q is defined as usual, assuming elastic scattering, as $q = (4\pi/\lambda)\sin(\theta/2)$, where θ is the angle between incident and scattered beam. Data were corrected for the empty cell signal and the solute and solvent incoherent background. A light water standard was used to normalize the scattered intensities to cm^{-1} units. The data was fitted with the DANSE software SasView. The SANS data for the S&S-type mixtures without additive[41] and with **BTA Achc**[39] have been reported previously. The number of molecules in the cross-section is calculated by assuming a distance of 3.62 Å between BTA monomers in the stacks.[55] The result of the fits for SANS analyses of **BTA C8** alone and additive-containing mixtures are summarized in Table 1.

NMR analyses: NMR spectra were recorded from JEOL JNM-ECZ400S spectrometer except for the mixture with $fs^0 = 9\%$ without additive (Figure 1d) which was recorded on a Bruker Avance 400 spectrometer. These spectrometers operate at a ^1H Larmor frequency of 400 MHz (400.2 MHz for the Bruker Avance 400 spectrometer) with a 5 mm broadband probe head ^1H /^{19}F/ ^{31}P -^{15}N (BBFO or Royal HFX probe). The ^1H NMR spectra were recorded using a pulse sequence of proton with a spectral width of 7183 Hz/6010 Hz, an acquisition time of 4.6 s/2.0 s, and a relaxation delay of 1 s/4 s for Bruker Avance 400 and JEOL JNM-ECZ400S spectrometers, respectively. Calibration was done on the residual solvent peak of C_7D_8 (^1H: 2.09 ppm). The ^{31}P NMR spectra were recorded using a pulse sequence $^{31}P\{^1H\}$ with a spectral width of 24300 Hz/65574 Hz, an acquisition time of 1.3 s/1.5 s, and a relaxation delay of 2 s for Bruker Avance 400 and JEOL JNM-ECZ400S spectrometers, respectively. A sample of H_3PO_4 85% in D_2O is used to calibrate the chemical shift reference at 0 ppm. The value of this reference is filled for each spectrum thus allowing their calibration.

Circular dichroism (CD) analyses: CD measurements were performed on a Jasco J-1500 spectrometer equipped with a Peltier thermostated cell holder and Xe laser. Data were recorded at 293 K with the following parameters: 50 nm.min^{-1} sweep rate, 0.05 nm data pitch, 2.0 nm bandwidth, and between 400 and 275 nm. Cylindrical spectrosil quartz cells of 0.10 mm pathlength (Starna® 31/Q/0.1) were used. For variable-temperature CD experiments, solutions were placed into cylindrical spectrosil quartz cells of 0.10 mm pathlength, heated to 373 K and the ellipticity was recorded at $\lambda =$ 295 nm during a cooling process down to 273 K (0.3 K.min^{-1}). All solutions were pre-heated before measurements. C_7D_8 and cell contributions at the same temperature were subtracted from the obtained signals. For all samples, LD contribution was negligible ($\Delta LD < 0.005$ dOD) and the shape of the CD signal was independent of the orientation of the quartz cells. Molar CD values are reported in L.mol^{-1}.cm^{-1} and are expressed as follows: $\Delta\varepsilon = \theta/(32982 \times l \times c)$ where θ is the measured ellipticity (mdeg), l is the optical path length in cm, and c is the concentration of **BTA P** in mol.L^{-1}.

UV-Vis analyses: UV-Vis absorption spectra were extracted from CD on each of the above samples and obtained after correction of the absorption of air, solvent, and cell at 293 K.

Catalytic experiments: A given amount of a stock solution prepared by mixing **BTA P** and $[Cu(OAc)_2 \cdot H_2O]$ was divided in order to get **BTA P** (6.9 mg, 10.0 μmol, 12 mol%) and $[Cu(OAc)_2 \cdot H_2O]$ (0.50 mg, 2.55 μmol, **BTA P**/[Cu] = 4, 3 mol%) in dry THF (500 μL) in each vial. The mixture was stirred for 30 minutes, the solvent was removed under vacuum and the tubes were kept under vacuum (10^{-3} mbar) for 1 hour. Then 4-nitroacetophenone (NPnone, 14.0 mg, 0.085 mmol, 100 mol%) was added before flushing the tube with argon for 10 seconds. A 10.0 mM stock solution of **BTA (*S*)-Cha** was prepared by mixing 11.7 mg of **BTA (*S*)-Cha** and 1.0 mL (867 mg) of toluene. Then 1.0 mM and 0.1 mM stock solutions were prepared by dilution. Then the desired quantity of **BTA (*S*)-Cha** monomers was introduced (values in parenthesis correspond to the quantity of **BTA (*S*)-Cha** and its final concentration in the solution): 86.7 mg of the 0.1 mM stock solution (0.01 μmol, 16 μM), 43.4 mg of the 1.0 mM stock solution (0.05 μmol, 80 μM), 86.7 mg of the 1.0 mM stock solution (0.10 μmol, 160 μM), 86.7 mg of the 10.0 mM stock solution (1.00 μmol, 1.6 mM), 238.4 mg of the 10.0 mM stock solution (2.75 μmol, 4.4 mM), 6.5 mg (5.53 μmol, 9.1 mM) of solid **BTA (*S*)-Cha** and 12.9 mg (11.0 μmol, 17.3 mM) of solid **BTA (*S*)-Cha**. Finally, achiral BTA additives when needed: **BTA C8** (5.4 mg, 10.0 μmol, 12.0 mol%), or **BTA Aib** (9.7 mg, 10.0 μmol, 12.0 mol%), or **BTA Acbc** (10.1 mg, 10.0 μmol, 12.0 mol%), or **BTA Cle** (10.5 mg, 10.0 μmol, 12.0 mol%), or **BTA Achc** (10.9 mg, 10.0 μmol, 12.0 mol%, for **BTA Achc**/**BTA P** = 1) and dry toluene were added to each vial in order to get a total volume of 600 μL. Samples were briefly heated up to solvent boiling point (≈383 K) and cooled down to room temperature. After cooling to 200 K, $PhSiH_3$ (21.0 μL, 0.17 mmol, 200 mol%) was added to each test tube, the tubes were manually shaken for homogenization, and the mixtures were stirred for 17 hours at 200 K. Typical work-up: Aqueous solution of HCl (10 wt%, 500 μL) was added at 200 K and the tubes were removed from the cooled container and let warmed to room temperature upon vigorous stirring until the solution became transparent. Then, the products were extracted with Et_2O (500 μL) and AcOEt (500 μL), the organic phases were collected and passed through a small silica plug. The solvents were evaporated and the crude material was analysed by ^1H NMR and by chiral GC. Conversion > 99% was obtained for all catalytic experiments, as determined by GC and ^1H NMR analyses. The optical purity was determined by chiral GC analysis. Chiral GC analyses: Chiral Cyclosil-B column, 30 m × 250 μm × 0.25 μm, inlet pressure = 12.6 psi. Injection temperature = 250 °C; detector temperature = 300 °C; column temperature = 145 °C. Retention times: 18 min (NPnone), 45 min ((*R*)-NPnol), 47 min ((S)-NPnol).[56]

Synthesis of BTA Acbc: In a flame-dried round-bottom flask, benzene-1,3,5-tricarbonyl chloride (0.8 g, 3.0 mmol, 1.0 equiv.) was dissolved in dry CH_2Cl_2 (100 mL) at room temperature under argon atmosphere. The dodecyl ester *p*-TsOH salt of Acbc (4.51 g, 9.9 mmol, 3.3 equiv.) was then added in one portion, and the resulting mixture was cooled to 0 °C with an ice/water bath. Dry NEt_3 (2.8 mL, 19.8 mmol, 6.6 equiv.) was then added dropwise, the reaction was let warmed to room temperature and stirred for 36 h. Brine was then added to the flask, and the crude mixture was extracted thrice with CH_2Cl_2. The combined organic phases were dried over $MgSO_4$, filtered, and the solvent was evaporated under reduced pressure. The product was then purified by flash column chromatography on silica gel, eluting with DCM/AcOEt 100:0–85:15 gradient yielding **BTA Acbc** as an off-white gum (1.90 g, 1.9 mmol, 63% yield). ^1H NMR (acetone-d_6): $\delta = 8.66$ (s, 3H), 8.40 (s, 3H), 4.13 (t, $^3J = 6.5$ Hz, 6H), 2.80–2.69 (m, 6H), 2.50–2.43 (m, 6H), 2.12–2.08 (m, 6H), 1.63 (pentet, $^3J = 6.5$ Hz, 6H), 1.40–1.18 (m, 54H), 0.88 ppm

Research Article
doi.org/10.1002/ceur.202300027

(t, $^3J = 7.2$ Hz, 9H). $^{13}C\{^1H\}$ NMR (acetone-d_6): $\delta = 173.72$, 166.06, 135.71, 129.66, 65.50, 59.89, 32.67, 32.10, 30.39, 30.32, 30.27, 30.10, 29.97, 26.68, 23.36, 16.34, 14.38 ppm. HRMS (ESI, *m/z*): Calculated for $C_{60}H_{99}N_3O_9Na$, $[M+Na]^+$: 1028.7274, found: 1028.7285. FTIR (ATR): 690 (m), 1106 (s), 1200 (s), 1302 (s), 1464 (w), 1540 (s), 1625 (s), 1736 (s), 2849 (s), 2926 (s), 3045 (w), 3215 cm^{-1} (br). **Synthesis of BTA Cle**: In a flame-dried round-bottom flask, benzene-1,3,5-tricarbonyl chloride (0.8 g, 3.0 mmol, 1.0 equiv.) was dissolved in dry CH_2Cl_2 (100 mL) at room temperature under argon atmosphere. The dodecyl ester *p*-TsOH salt of Cle (4.64 g, 9.9 mmol, 3.3 equiv.) was then added in one portion, and the resulting mixture was cooled to 0 °C with an ice/water bath. Dry NEt_3 (2.8 mL, 19.8 mmol, 6.6 equiv.) was then added dropwise, the reaction was let warmed to room temperature and stirred for 36 h. Brine was then added to the flask, and the crude mixture was extracted thrice with CH_2Cl_2. The combined organic phases were dried over $MgSO_4$, filtered, and the solvent was evaporated under reduced pressure. The product was then purified by flash column chromatography on silica gel, eluting with DCM/AcOEt 100:0–85:15 gradient yielding **BTA Cle** as an off-white gum (1.92 g, 1.8 mmol, 61% yield). ^1H NMR (acetone-d_6): $\delta = 8.37$ (s, 3H), 8.34 (s, 3H), 4.08 (t, $^3J = 6.5$ Hz, 6H), 2.36–2.29 (m, 6H), 2.21–2.13 (m, 6H), 1.90-1.74 (m, 12H), 1.59 (pentet, $^3J = 6.5$ Hz, 6H), 1.40–1.12 (m, 54H), 0.88 ppm (t, $^3J = 7.2$ Hz, 9H). $^{13}C\{^1H\}$ NMR (acetone-d_6): $\delta = 174.44$, 166.48, 135.89, 129.65, 67.42, 65.40, 37.70, 32.67, 30.40, 30.38, 30.31, 30.25, 30.10, 29.96, 26.70, 25.24, 23.36, 14.38 ppm. HRMS (ESI, *m/z*): Calculated for $C_{63}H_{105}N_3O_9Na$, $[M+Na]^+$: 1070.7743, found: 1070.7749. FTIR (ATR): 690 (m), 1039 (w), 1167 (s), 1319 (w), 1459 (w), 1550 (s), 1634 (s), 1736 (s), 2851 (s), 2919 (s), 3056 (w), 3221 cm^{-1} (br).

Acknowledgements

The French Agence Nationale de la Recherche is acknowledged for funding the project AbsoluCat (ANR-17-CE07-0002, PhD position of AH). This work was supported by the China Scholarship Council (CSC, PhD grants of Y.L. and H. K.). Jacques Jestin (LLB, Saclay) is acknowledged for assistance with SANS experiment. The GDR 3712 Chirafun is acknowledged for allowing a collaborative network.

Conflict of Interests

The authors declare no conflict of interest.

Data Availability Statement

The data that support the findings of this study are available in the supplementary material of this article.

Keywords: achiral additive · benzene-1,3,5-tricarboxamide (BTA) · coassembly · induction of chirality · "sergeants-and-soldiers" effect · supramolecular polymers · terpolymer

[1] T. F. A. De Greef, M. M. J. Smulders, M. Wolffs, A. P. H. J. Schenning, R. P. Sijbesma, E. W. Meijer, *Chem. Rev.* **2009**, *109*, 5687–5754.
[2] L. Yang, X. Tan, Z. Wang, X. Zhang, *Chem. Rev.* **2015**, *115*, 7196–7239.
[3] M. F. J. Mabesoone, A. R. A. Palmans, E. W. Meijer, *J. Am. Chem. Soc.* **2020**, *142*, 19781–19798.
[4] T. Aida, E. W. Meijer, *Isr. J. Chem.* **2020**, *60*, 33–47.
[5] B. Adelizzi, N. J. Van Zee, L. N. J. de Windt, A. R. A. Palmans, E. W. Meijer, *J. Am. Chem. Soc.* **2019**, *141*, 6110–6121.
[6] Z. Huang, B. Qin, L. Chen, J.-F. Xu, C. F. J. Faul, X. Zhang, *Macromol. Rapid Commun.* **2017**, *38*, 1700312.
[7] J. Matern, Y. Dorca, L. Sánchez, G. Fernández, *Angew. Chem. Int. Ed.* **2019**, *58*, 16730–16740.
[8] C. Wang, L. Xu, L. Zhou, N. Liu, Z.-Q. Wu, *Angew. Chem. Int. Ed.* **2022**, *61*, e202207028.
[9] M. Hartlieb, E. D. H. Mansfield, S. Perrier, *Polym. Chem.* **2020**, *11*, 1083–1110.
[10] C. Rest, R. Kandanelli, G. Fernández, *Chem. Soc. Rev.* **2015**, *44*, 2543–2572.
[11] C. Kulkarni, E. W. Meijer, A. R. A. Palmans, *Acc. Chem. Res.* **2017**, *50*, 1928–1936.
[12] A. R. A. Palmans, E. W. Meijer, *Angew. Chem. Int. Ed.* **2007**, *46*, 8948–8968.
[13] M. Liu, L. Zhang, T. Wang, *Chem. Rev.* **2015**, *115*, 7304–7397.
[14] E. Yashima, N. Ousaka, D. Taura, K. Shimomura, T. Ikai, K. Maeda, *Chem. Rev.* **2016**, *116*, 13752–13990.
[15] H. Gu, Y. Nakamura, T. Sato, A. Teramoto, M. M. Green, S. K. Jha, C. Andreola, M. P. Reidy, *Macromolecules* **1998**, *31*, 6362–6368.
[16] S. Cantekin, T. F. A. de Greef, A. R. A. Palmans, *Chem. Soc. Rev.* **2012**, *41*, 6125–6137.
[17] Y. Dorca, J. Matern, G. Fernández, L. Sánchez, *Isr. J. Chem.* **2019**, *59*, 869–880.
[18] M. M. J. Smulders, I. A. W. Filot, J. M. A. Leenders, P. van der Schoot, A. R. A. Palmans, A. P. H. J. Schenning, E. W. Meijer, *J. Am. Chem. Soc.* **2010**, *132*, 611–619.
[19] A. Das, G. Vantomme, A. J. Markvoort, H. M. M. ten Eikelder, M. Garcia-Iglesias, A. R. A. Palmans, E. W. Meijer, *J. Am. Chem. Soc.* **2017**, *139*, 7036–7044.
[20] G. Vantomme, G. M. ter Huurne, C. Kulkarni, H. M. M. ten Eikelder, A. J. Markvoort, A. R. A. Palmans, E. W. Meijer, *J. Am. Chem. Soc.* **2019**, *141*, 18278–18285.
[21] E. Weyandt, G. M. ter Huurne, G. Vantomme, A. J. Markvoort, A. R. A. Palmans, E. W. Meijer, *J. Am. Chem. Soc.* **2020**, *142*, 6295–6303.
[22] E. Weyandt, L. Leanza, R. Capelli, G. M. Pavan, G. Vantomme, E. W. Meijer, *Nat. Commun.* **2022**, *13*, 248.
[23] E. Weyandt, M. F. J. Mabesoone, L. N. J. de Windt, E. W. Meijer, A. R. A. Palmans, G. Vantomme, *Org. Mat.* **2020**, *02*, 129–142.
[24] M. A. Martínez-Aguirre, Y. Li, N. Vanthuyne, L. Bouteiller, M. Raynal, *Angew. Chem. Int. Ed.* **2021**, *60*, 4183–4191.
[25] R. van Buel, D. Spitzer, C. M. Berac, P. van der Schoot, P. Besenius, S. Jabbari-Farouji, *J. Chem. Phys.* **2019**, *151*, 014902.
[26] B. Adelizzi, A. Aloi, A. J. Markvoort, H. M. M. Ten Eikelder, I. K. Voets, A. R. A. Palmans, E. W. Meijer, *J. Am. Chem. Soc.* **2018**, *140*, 7168–7175.
[27] H. Su, S. A. H. Jansen, T. Schnitzer, E. Weyandt, A. T. Rösch, J. Liu, G. Vantomme, E. W. Meijer, *J. Am. Chem. Soc.* **2021**, *143*, 17128–17135.
[28] R. Liao, F. Wang, Y. Guo, Y. Han, F. Wang, *J. Am. Chem. Soc.* **2022**, *144*, 9775–9784.
[29] K. M. Vonk, E. W. Meijer, G. Vantomme, *Chem. Sci.* **2021**, *12*, 13572–13579.
[30] P. Xing, Y. Zhao, *Acc. Chem. Res.* **2018**, *51*, 2324–2334.
[31] P. Besenius, *J. Polym. Sci. Part A* **2017**, *55*, 34–78.
[32] N. J. Van Zee, B. Adelizzi, M. F. J. Mabesoone, X. Meng, A. Aloi, R. H. Zha, M. Lutz, I. A. W. Filot, A. R. A. Palmans, E. W. Meijer, *Nature* **2018**, *558*, 100–103.
[33] N. J. Van Zee, M. F. J. Mabesoone, B. Adelizzi, A. R. A. Palmans, E. W. Meijer, *J. Am. Chem. Soc.* **2020**, *142*, 20191–20200.
[34] A. K. Mondal, M. D. Preuss, M. L. Ślęczkowski, T. K. Das, G. Vantomme, E. W. Meijer, R. Naaman, *J. Am. Chem. Soc.* **2021**, *143*, 7189–7195.
[35] M. D. Preuss, S. A. H. Jansen, G. Vantomme, E. W. Meijer, *Isr. J. Chem.* **2021**, *61*, 622–628.
[36] A. Desmarchelier, X. Caumes, M. Raynal, A. Vidal-Ferran, P. W. N. M. van Leeuwen, L. Bouteiller, *J. Am. Chem. Soc.* **2016**, *138*, 4908–4916.
[37] J. M. Zimbron, X. Caumes, Y. Li, C. M. Thomas, M. Raynal, L. Bouteiller, *Angew. Chem. Int. Ed.* **2017**, *56*, 14016–14019.
[38] Y. Li, X. Caumes, M. Raynal, L. Bouteiller, *Chem. Commun.* **2019**, *55*, 2162–2165.
[39] Y. Li, A. Hammoud, L. Bouteiller, M. Raynal, *J. Am. Chem. Soc.* **2020**, *142*, 5676–5688.

Research Article
doi.org/10.1002/ceur.202300027

[40] P. Aoun, A. Hammoud, M. A. Martínez-Aguirre, L. Bouteiller, M. Raynal, *Catal. Sci. Technol.* **2022**, *12*, 834–842.
[41] A. Hammoud, Y. Li, M. A. Martinez-Aguirre, H. Kong, L. Dubreucq, C. Troufflard, L. Bouteiller, M. Raynal, *Chem. Eur. J.* **2023**, e202300189.
[42] M. M. J. Smulders, P. J. M. Stals, T. Mes, T. F. E. Paffen, A. P. H. J. Schenning, A. R. A. Palmans, E. W. Meijer, *J. Am. Chem. Soc.* **2010**, *132*, 620–626.
[43] A. Desmarchelier, M. Raynal, P. Brocorens, N. Vanthuyne, L. Bouteiller, *Chem. Commun.* **2015**, *51*, 7397–7400.
[44] A. Desmarchelier, B. G. Alvarenga, X. Caumes, L. Dubreucq, C. Troufflard, M. Tessier, N. Vanthuyne, J. Idé, T. Maistriaux, D. Beljonne, P. Brocorens, R. Lazzaroni, M. Raynal, L. Bouteiller, *Soft Matter* **2016**, *12*, 7824–7838.
[45] A. J. Metrano, A. J. Chinn, C. R. Shugrue, E. A. Stone, B. Kim, S. J. Miller, *Chem. Rev.* **2020**, *120*, 11479–11615.
[46] X. Caumes, A. Baldi, G. Gontard, P. Brocorens, R. Lazzaroni, N. Vanthuyne, C. Troufflard, M. Raynal, L. Bouteiller, *Chem. Commun.* **2016**, *52*, 13369–13372.
[47] The difference in intensity between those spectra is attributed to the fact that the FTIR spectrum of **BTA Aib** (5.8 mM) in methylcyclohexane (reference [44]) has been used as an imperfect blueprint of the FTIR signals of **BTA Achc** monomers in stacks.
[48] Kuhn anisotropy factor (g), is defined as $g = \theta/(32982 \times Abs)$ where θ and Abs are the ellipticity and UV/Vis absorbance measured at $\lambda =$ 295 nm, from the CD and UV-Vis spectra, respectively.
[49] The screw sense excesses ($se = g_{exp}/g_{max}$, assuming a g_{max} value of 7×10^{-4}) and *e.e.* values (expected *e.e.* = se × *e.e.*max) can be compared as follows (the *e.e.* max value was deduced from the *e.e.* plateau and thus slightly varies depending on the mixtures): additive-free mixture ($g = 2.9 \times 10^{-4}$, se = 40%, expected *e.e.* = 39%, measured *e.e.* = 55%), **BTA C8** mixture ($g = 4.1 \times 10^{-4}$, se = 59%, expected *e.e.* = 51%, measured *e.e.* = 61%) and **BTA Achc** mixture ($g = 7.2 \times 10^{-4}$, se = 100%, expected *e.e.* = 82%, measured *e.e.* = 84%). The slight differences might come from the different temperatures for the CD (293 K) and catalytic experiments (200 K) or slightly different scaling factors between *e.e.* and g values (see reference [24]).
[50] L. Hong, W. Sun, D. Yang, G. Li, R. Wang, *Chem. Rev.* **2016**, *116*, 4006–4123.
[51] M. F. J. Mabesoone, G. M. ter Huurne, A. R. A. Palmans, E. W. Meijer, *J. Am. Chem. Soc.* **2020**, *142*, 12400–12408.
[52] Y. Li, L. Bouteiller, M. Raynal, *ChemCatChem* **2019**, *11*, 5212–5226.
[53] For a discussion of the notion of defects in supramolecular polymers, see: A. Jangizehi, F. Schmid, P. Besenius, K. Kremer, S. Seiffert, *Soft Matter* **2020**, *16*, 10809–10859.
[54] P. J. M. Stals, M. M. J. Smulders, R. Martín-Rapún, A. R. A. Palmans, E. W. Meijer, *Chem. Eur. J.* **2009**, *15*, 2071–2080.
[55] M. P. Lightfoot, F. S. Mair, R. G. Pritchard, J. E. Warren, *Chem. Commun.* **1999**, 1945–1946.
[56] G. Uray, W. Stampfer, W. M. F. Fabian, *J. Chromatogr. A* **2003**, *992*, 151–157.

Manuscript received: April 20, 2023
Version of record online: June 22, 2023